



## The 65th ASH Annual Meeting Abstracts

## POSTER ABSTRACTS

## 803.EMERGING TOOLS, TECHNIQUES AND ARTIFICIAL INTELLIGENCE IN HEMATOLOGY

**Microfluidic Assessment of T Cell Deformability and Capillary Network Occlusion**Somin Jung<sup>1</sup>, William J. Wulftange, MSc,BS<sup>1</sup>, Payam Fadaei, MSc<sup>1</sup>, Yuncheng Man, PhD<sup>1</sup>, Umut A. Gurkan, PhD<sup>1</sup><sup>1</sup> Case Western Reserve University, Cleveland, OH

**Introduction:** Adoptive T cell therapies offer a new frontier of cancer treatment that disrupts the conventional chemotherapy paradigm. Naïve T cells can be genetically modified to directly target cancerous cells and have proven to be aggressively effective in fighting cancers resistant to chemotherapies. A major challenge that adoptive T cell therapies face is successfully delivering the cell products to the location of the target cells, which is particularly challenging in the case of solid tumors. A complete characterization of the biomechanical properties of T cell products would help researchers gain insight into the capacity of these engineered cells to navigate and extravasate through vasculature and tumor microenvironments. Previous studies have found that T cell volume, cortical tension, and dynamic resistance increase with activation (Waugh *et al. Front Bioeng Biotechnol.* 2023). A simple and reproducible method to easily quantify and assess such cellular properties has yet to be established. Presently, we describe a microfluidic assay for the rapid and robust characterization of the mechanical changes of T cells upon activation. Our assay models the microcapillaries through a gradient of micropillar arrays, which allows for the evaluation of T cells perfused through the network. The spacing between pillars is 12  $\mu\text{m}$  at the first array, similar to small arterioles, and incrementally decreases to 3  $\mu\text{m}$  spacing in the last array, mimicking small capillaries ( **Figure 1A**). Trafficking of adoptive T cell therapies through the microvasculature networks of this scale into their target tissues represents a persistent and major challenge facing these therapies (Marofi *et al. Stem Cell Res. Ther.* 2021).

**Methods:** The microfluidic devices were fabricated by casting polydimethylsiloxane (PDMS) on a silicone wafer fabricated through photolithographic protocols. Devices contain arrays of pillars measuring 20  $\mu\text{m}$  x 10  $\mu\text{m}$  x 12  $\mu\text{m}$  with gradient spacing beginning at 12  $\mu\text{m}$  at the inlet and 3  $\mu\text{m}$  at the outlet. Jurkat T cells were cultured in RPMI 1640 medium with 10% fetal bovine serum and used in a naïve state or activated via antibody stimulation of CD3 and CD28. T cells were then suspended in growth media at  $1 \times 10^6$  cells/mL. Microchannels were wetted and cleaned with 100% ethanol perfused at 10  $\mu\text{L}/\text{min}$  for 15 minutes followed by cell culture media at 10  $\mu\text{L}/\text{min}$  for 15 minutes to block the non-specific binding sites on the PDMS and to create a biocompatible environment for the cell sample. The devices were connected to a digital pneumatic pressure-based flow pump system. The cell sample was perfused at 100 mBar for 7 minutes and a subsequent wash process with growth media at 100 mBar for 7 minutes was performed to flush non-occluded cells. Upon completion of the experiment, the channel was scanned using Phase and DAPI filters with an Olympus IX83 inverted motorized microscope, and occluded T cells were quantified using ImageJ.

**Results:** Our assay showed distinct levels of T cell occlusion upon activation through CD3 and CD28 stimulation. Naïve T cells showed lower levels of occlusion in each of the first five arrays compared to activated T cells, while both groups showed high levels of occlusion in the final 3  $\mu\text{m}$  array. Activated T cells showed approximately three times the amount of occlusion in the second through fifth arrays. To assess overall occlusion, we use the Occlusion Index (OI), which considers the density of pillars and the number of cells caught in each array. We found that activated T cells had a significantly higher OI when compared to non-activated T cell samples ( $p < 0.05$ , unpaired *t*-test). Naïve T cells had an OI mean of  $24.4 \pm 5.0$  while activated T cells had a mean of  $42.5 \pm 5.6$  ( **Figure 1B**).

**Conclusions:** Our results show that there is a significant increase in resistance of activated T cells through a microvasculature-modeled environment compared to their naïve counterparts. As adoptive T cell therapies increase in popularity, a complete understanding of the biomechanical properties of these cell products will be necessary for effective design. Our microfluidic assay mimics the narrowing channels of the microvasculature and permits the study of how naïve and engineered T cells travel through these mechanically challenging spaces.

**Disclosures Gurkan:** Xatek Inc.: Current holder of stock options in a privately-held company, Patents & Royalties; Hemex Health Inc.: Current Employment, Current holder of stock options in a privately-held company, Patents & Royalties, Research

Funding; *BioChip Labs Inc*: Current Employment, Current holder of stock options in a privately-held company, Patents & Royalties, Research Funding; *DxNow Inc.*: Current holder of stock options in a privately-held company, Patents & Royalties.

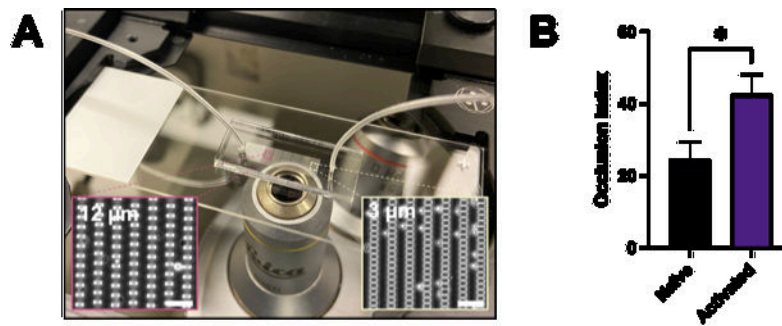


**Figure 1. T cells exhibit decreased deformability upon activation in microscale flow. (A)** Image of the micropillar-based microfluidic deformability assay. Macro images of the first array with 12  $\mu\text{m}$  spacing and the last array with 3  $\mu\text{m}$  spacing are shown. Scale bars represent 50  $\mu\text{m}$ . **(B)** Activated T cells exhibit lower deformability compared to naïve counterparts. Occlusion Index accounts for the number of cells occluded in each array over the entire device. Naïve T cells had an OI mean of  $24.4 \pm 5.0$  while activated T cells had a mean of  $42.5 \pm 5.6$ . ( $p < 0.05$ , unpaired  $t$ -test).

Figure 1

<https://doi.org/10.1182/blood-2023-187442>